JOURNAL OF GUIDANCE, CONTROL, AND DYNAMICS
Vol. 24, No. 2, March–April 2001

Required Ranges for Conflict Resolutions in Air Traffic Management

Vincent H. Kuo* and Yiyuan J. Zhao†
University of Minnesota, Minneapolis, Minnesota 55455

To maintain sufficient separation between two aircraft, either one or both aircraft must initiate avoidance maneuvers when their relative range approaches a certain limit before minimum separation standards are violated. This limit is defined as the required range for conflict resolutions. A two-step procedure based on optimization methods is presented for calculating required ranges. First, a nonlinear optimal control problem is used to determine the minimum range for a given relative heading angle of the intruder aircraft, at which immediate avoidance maneuvers starting from this point onward would just be sufficient to maintain the minimum separation standards. Then, the required range for conflict resolutions is estimated by finding the largest minimum range over all meaningful relative heading angles of the intruder aircraft. Point-mass aircraft models of a typical commercial aircraft are used. Both cooperative and noncooperative maneuvers are studied. The nonlinear optimal control problems are converted into parameter optimizations via a collocation approach for numerical solutions. Required ranges are calculated for the individual uses of heading control, speed control, and altitude control.

Nomenclature

A	=	a matrix
a, b	=	horizontal and vertical separation requirements, respectively
C_{D_0}	=	parasite drag coefficient
C_L, C_D	=	lift and drag coefficients, respectively
$c(X)$	=	nonlinear vector function of X
D	=	aerodynamic drag
$\boldsymbol{f}, f$	=	generic function
g	=	gravitational acceleration
h	=	inertial altitude
h_k	=	length of time subintervals
K	=	drag polar coefficient
L	=	aerodynamic lift
$\boldsymbol{L}_b$	=	lower bound vector
M	=	Mach number
m	=	aircraft mass, number of control variables
N	=	number of nodes for NPSOL
n	=	number of state variables
R	=	range between two aircraft
r	=	relative range in the horizontal plane
S	=	aircraft reference area
T	=	engine thrust
t	=	time
$\boldsymbol{U}_b$	=	upper bound vector
$\boldsymbol{u}$	=	generic control vector
V	=	airspeed
V_c	=	characteristic speed
W	=	aircraft weight
$\boldsymbol{X}$	=	solution parameter vector
x, y	=	east and north positions, respectively
$\boldsymbol{x}$	=	generic state vector
z_1, z_2, z	=	defined variables
β	=	bearing angle
γ	=	air-relative flight-path angle
$\Delta( )$	=	$( )_2 - ( )_1$
η	=	a defined constant
Θ	=	elevation angle
κ	=	thrust setting
ρ	=	air density
τ	=	normalized time
ϕ	=	bank angle
Ψ	=	heading angle of the range vector
ψ	=	air-relative velocity heading
ψ_r	=	relative heading angle

Subscripts

CR	=	cruising conditions
f	=	final value
0	=	initial value
1	=	own aircraft
2	=	intruder aircraft

Superscripts

$\dot{}$	=	time derivative
$'$	=	derivative with respect to normalized time
$\bar{}$	=	normalized variable

Received 14 February 2000; revision received 17 May 2000; accepted for publication 26 May 2000.

*Graduate Student; currently Senior Research Scientist, Stavatti Corporation, 520 Airport Road, St. Paul, MN 55075.

†Associate Professor, Aerospace Engineering and Mechanics; gyyz@aem.umn.edu. Senior Member AIAA.

Introduction

THE nation's air traffic control (ATC) system is responsible for maintaining separations among all aircraft following instrument flight rules.[1] ATC facilities under the jurisdiction of the Federal Aviation Administration (FAA) employ about 20,000 controllers nationwide and handle about 170,000 aircraft operations per day. Air traffic has increased significantly over the last several decades and is expected to grow further. Growth in air traffic has severely burdened both the existing air traffic control infrastructure and the air traffic controllers.

The current ATC system maintains aircraft separations through pilot adherence to predefined routes and flight procedures and controller interventions. In the recently proposed concept of a free-flight environment for future air traffic management,[2] aircraft operators can change flight paths in real time to achieve the optimal efficiency for the aircraft. Air traffic controllers are only supposed to intervene to resolve potential conflicts among aircraft.

For both the current and future air traffic systems, aircraft must be sufficiently separated from one another. Currently, the FAA specifies that any two aircraft in high-altitude en route airspace must be separated by at least 2000 ft vertically or 5 n mile horizontally. The horizontal requirement becomes 3 n mile over terminal areas, and the vertical requirement becomes 1000 ft below flight level 290 (29,000 ft). These requirements constitute the minimum separation standards at the present time.

In general, the minimum separation standards are affected by accuracies of navigation and surveillance, by controller/pilot response and communication delays, by response times of aircraft maneuvers, by winds aloft, and by characteristics of aircraft turbulent wake vortices. The current minimum separation standards are designed to ensure a sufficient margin of safety even with the largest likely error in each component of the ATC system. The minimum separation standards will likely be decreased over time, due to advances in aircraft communication, navigation, and surveillance, as well as increased understanding of aircraft wake vortices.

Because of the finite time needed to change aircraft flight states, the execution of conflict resolution maneuvers requires a sufficient space to be successful. In other words, proper conflict avoidance maneuvers must be started when the relative range between two aircraft approaches a certain boundary, before the minimum separation standards are violated. Of course, individual aircraft can always start avoidance maneuvers in advance of this range boundary, when a potential conflict is detected.

This paper introduces the concept of required range for conflict resolutions at which conflict avoidance maneuvers become necessary. A two-step procedure based on optimization methods is presented for calculating required ranges for pairwise conflict resolutions. Specifically, nonlinear optimal control problems are first used to determine minimum ranges between two aircraft at which correct conflict resolution maneuvers must be initiated to avoid potential conflicts under specified aircraft flight conditions. These minimum ranges are functions of the relative heading angle and the bearing angle of the intruder aircraft, the type of control authority used for conflict resolutions, and other aircraft flight conditions. Then, the required range is determined as the largest of these minimum ranges over all likely relative heading angles of the intruder aircraft. Therefore, the required range concept offers a somewhat conservative description of the necessary range required for performing successful conflict resolution maneuvers. It can play roles similar to the concept of an alert zone, which is a time-based region of airspace that is used to indicate a condition where intervention may be necessary.[2] Knowledge of required ranges can reveal the effectiveness of different conflict resolution strategies and control authorities.

In this paper, point-mass aircraft models of typical commercial aircraft with a single control authority are used. Aircraft control is assumed to be heading, speed, or altitude. The formulated optimal control problems are converted to parameter optimizations via a collocation approach for numerical solutions. Both cooperative maneuvers and noncooperative maneuvers are examined.

In the past, algorithms have been studied and used for automatic detection and resolution of aircraft conflicts in practical applications. The Center/TRACON Automation System (CTAS) developed at NASA Ames Research Center can assist air traffic controllers by providing computer-generated flight advisories.[3–7] These advisories, consisting of speed, heading, and altitude instructions to the pilots, guarantee safe separations among all aircraft and produce an expeditious flow of traffic. In particular, CTAS detects and provides options for resolving potential conflicts.[8–14] In comparison, the Traffic Alert and Collision Avoidance System (TCAS)[15–18] was developed for onboard use by individual aircraft. TCAS senses the presence of nearby aircraft by interrogating the transponders carried by other aircraft. When TCAS senses that a nearby aircraft is a possible collision threat, it issues a traffic advisory to the pilot indicating the presence and location of the other aircraft. If the encounter becomes hazardous, TCAS can issue a maneuver advisory for collision avoidance. Advanced versions of TCAS are still under development.

In addition, there has been extensive research on determining strategies and algorithms for aircraft conflict detection and resolution.[19–30] In particular, nonlinear optimal control theories are used to determine conflict avoidance maneuvers.[31–36] Compared with the past work, the current paper focuses on ranges required for conflict resolutions, rather than specific strategies for conflict resolutions. In this regard, the potential use of optimal control theories in estimating alert zones is mentioned in Ref. 32.

This paper focuses on two-aircraft conflict scenarios. The majority of potential conflicts in the current air traffic system involve two aircraft at a time. Whether the probability of multiple-aircraft conflicts would be higher in the proposed free-flight concept is still being studied. Regardless, a clear understanding of two-aircraft conflict scenarios is fundamentally important to the development of conflict resolution strategies for multiple aircraft.

Modeling of Aircraft Dynamics and Separation Standards

Required ranges for conflict resolutions can be conveniently described from an airborne point of view. Therefore, relative equations of motion of one aircraft with respect to another are used. Figure 1 shows the three-dimensional geometry of an intruder aircraft (AC_2) with respect to the own aircraft (AC_1). The AC_1 and the AC_2 are considered point masses with airspeed vectors $\boldsymbol{V}_1$ and $\boldsymbol{V}_2$, respectively. The orientation of an airspeed vector $\boldsymbol{V}$ can be specified by the air-relative flight-path angle γ and the heading angle ψ. The air-relative flight-path angle is the angle between the airspeed vector and the local horizon and is positive when the aircraft climbs. The heading angle is measured from the north to the projection of the airspeed vector onto the local horizontal plane.

With respect to AC_1, the orientation of AC_2 can be described by the relative heading angle and the bearing angle,

$$\psi_r = \psi_2 - \psi_1 \tag{1}$$

$$\beta = \Psi - \psi_1 \tag{2}$$

In this paper, it is assumed

$$-180 \le \beta \le 180 \qquad 0 \le \psi_r \le 360 \tag{3}$$

with angles in degrees.

Point-mass equations of motion for a single commercial aircraft under the flat Earth assumption can be found in Ref. 37. The relative coordinates of AC_2 with respect to AC_1 relate to differences in inertial positions of the two aircraft through

$$R\cos\Theta\sin\Psi = x_2 - x_1 \triangleq \Delta x \tag{4}$$

$$R\cos\Theta\cos\Psi = y_2 - y_1 \triangleq \Delta y \tag{5}$$

$$R\sin\Theta = h_2 - h_1 \triangleq \Delta h \tag{6}$$

To obtain relative equations of motion of AC_2 with respect to AC_1, one can differentiate Eqs. (4–6) and solve for $\dot{R}$, $\dot{\Psi}$, and $\dot{\Theta}$. By the neglecting of relative wind components, a set of general equations of motion for the two aircraft are given as

$$\dot{R} = -V_1[\cos\Theta\cos(\Psi - \psi_1)\cos\gamma_1 + \sin\Theta\sin\gamma_1] + V_2[\cos\Theta\cos(\Psi - \psi_2)\cos\gamma_2 + \sin\Theta\sin\gamma_2] \tag{7}$$

$$R\cos\Theta\dot{\Psi} = V_1\sin(\Psi - \psi_1)\cos\gamma_1 - V_2\sin(\Psi - \psi_2)\cos\gamma_2 \tag{8}$$

$$R\dot{\Theta} = V_1[\sin\Theta\cos(\Psi - \psi_1)\cos\gamma_1 - \cos\Theta\sin\gamma_1] - V_2[\sin\Theta\cos(\Psi - \psi_2)\cos\gamma_2 - \cos\Theta\sin\gamma_2] \tag{9}$$

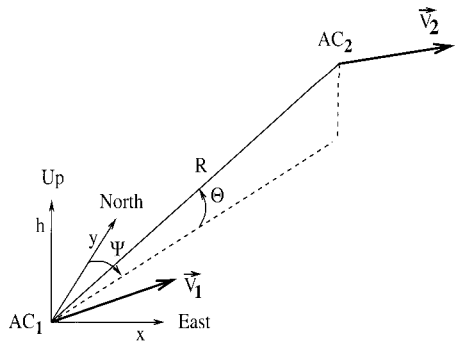

Fig. 1 Two-aircraft conflict geometry.

$$m_1\dot{V}_1 = T_1 - D_1 - m_1 g \sin\gamma_1 \tag{10}$$

$$m_1 V_1 \cos\gamma_1 \dot{\psi}_1 = L_1 \sin\phi_1 \tag{11}$$

$$m_2\dot{V}_2 = T_2 - D_2 - m_2 g \sin\gamma_2 \tag{12}$$

$$m_2 V_2 \cos\gamma_2 \dot{\psi}_2 = L_2 \sin\phi_2 \tag{13}$$

$$\dot{x}_1 = V_1 \cos\gamma_1 \sin\psi_1 \tag{14}$$

$$\dot{y}_1 = V_1 \cos\gamma_1 \cos\psi_1 \tag{15}$$

$$\dot{h}_1 = V_1 \sin\gamma_1 \tag{16}$$

where

$$L = \tfrac{1}{2}\rho V^2 S C_L \tag{17}$$

$$D = \tfrac{1}{2}\rho V^2 S C_D \tag{18}$$

$$C_D = C_{D_0} + K C_L^2 \tag{19}$$

In the following, required ranges for conflict resolutions are calculated for the use of single control authorities. Simplified equations of motion and constraints are discussed in specific cases. For good numerical efficiencies, all variables are normalized by proper combinations of a characteristic speed V_c and the acceleration of gravity, g. We have

$$\bar{V} = \frac{V}{V_c} \qquad \bar{R}, \bar{x}, \bar{y}, \bar{h} = \frac{R, x, y, h}{V_c^2/g}$$

$$\tau = \frac{t}{V_c/g} \qquad ()' \triangleq \frac{\mathrm{d}()}{\mathrm{d}\tau} = \frac{V_c}{g}\frac{\mathrm{d}()}{\mathrm{d}t} \tag{20}$$

To obtain specific numerical results, aircraft characteristics based on a typical commercial aircraft model derived in Ref. 38 are used. The major parameters of this aircraft model are as follows: $(T_{\max}/W)_{CR} = 0.087$, $K = 0.057$, $C_{D_0} = 0.019$, $\rho_{CR} = 7.38 \times 10^{-4}$ slugs/ft^3, $W/S = 106.8$ psf, $M_{CR} = 0.8$, and $V_{CR} = 461.2$ kn. A typical cruise flight phase is considered.

The current definitions of minimum separation standards are simple to conceptualize but difficult to use in optimization studies. Optimization methods often use gradient information and, thus, prefer smooth functions. An ellipsoidal approximation to these separation standards was proposed in Ref. 39. In this smooth approximation, each aircraft is centered inside a hypothetical conflict ellipsoid with semimajor axis a and semiminor axis b. For en route flights over flight level 290, $a = 5$ n mile and $b = 2000$ ft. Any other aircraft penetrating this hypothetical ellipsoid can be considered as causing a conflict. Using this ellipsoidal approximation, the conflict-free requirement is given by

$$[(\Delta x)^2 + (\Delta y)^2]/a^2 + [(\Delta h)^2/b^2] \geq 1 \tag{21}$$

or from Eqs. (4–6)

$$R(t) \geq ab \Big/ \sqrt{a^2 \sin^2\Theta + b^2 \cos^2\Theta} \tag{22}$$

For coaltitude level flights, $\Theta = 0$, and the conflict-free requirement becomes $R(t) \geq a$.

Two types of conflict avoidance maneuvers are considered. In a cooperative maneuver, both aircraft try to avoid each other's protected zones. In a noncooperative maneuver, only AC_1 tries to avoid AC_2, whereas AC_2 maintains its original flight path. The case where AC_2 may accidentally maneuver to cause a conflict is not included here.

Numerical Solutions of Optimal Control Problems

A generic optimal control problem in this paper seeks to determine the optimal final time t_f and the control history $\boldsymbol{u}(t)$ from

$$\min_{u(t),t_f} I = \phi[\boldsymbol{x}(t_0)] \tag{23}$$

subject to

$$\dot{\boldsymbol{x}} = \boldsymbol{f}[\boldsymbol{x}(t), \boldsymbol{u}(t), t] \tag{24}$$

$$\boldsymbol{\varphi}[\boldsymbol{x}(t_0), t_0] \geq 0 \tag{25}$$

$$\boldsymbol{S}[\boldsymbol{x}(t), \boldsymbol{u}(t), t] \geq 0 \tag{26}$$

$$\boldsymbol{\psi}[\boldsymbol{x}(t_f), t_f] \geq 0 \tag{27}$$

where ϕ is a scalar cost function, $\boldsymbol{\varphi}$ contains constraints at the initial time, $\boldsymbol{S}$ contains various path constraints, and $\boldsymbol{\psi}$ contains terminal constraints.[40] In general, $\boldsymbol{\varphi}$, $\boldsymbol{S}$, and $\boldsymbol{\psi}$ are vectors.

An effective approach to solving nonlinear optimal control problems is to convert them into parameter optimizations.[41–43] In particular, the collocation method parameterizes both state and control variables into parameters and is highly flexible. In a collocation method, the time interval of solution is divided into a series of N user-selected nodes (or time points):

$$t_0 = t_1 < t_2 < \cdots < t_k < \cdots < t_N = t_f \tag{28}$$

which can be either equally or variably spaced. Define for $k = 1, \ldots, N-1$,

$$h_k = t_{k+1} - t_k \tag{29}$$

At each node t_k, we discretize both the state and control variables. Figure 2 shows the discretization of state variables. The corresponding discretized variables are represented by

$$x_1^i, \ldots, x_k^i, \ldots, x_N^i \tag{30}$$

$$u_1^j, \ldots, u_k^j, \ldots, u_N^i \tag{31}$$

where $x_k^i = x^i(t_k)$ is the ith component of the state vector $\boldsymbol{x}$ evaluated at t_k and $u_k^j = u^j(t_k)$ is the jth component of the control vector $\boldsymbol{u}$ evaluated at t_k, $i = 1, \ldots, n$, $j = 1, \ldots, m$, and $k = 1, \ldots, N$.

There are many ways to approximate the dynamic equation in Eq. (24). In this paper, it is enforced at the midinterval points through Simpson's one-third rule (see Ref. 43),

$$\boldsymbol{x}_{k+1} = \boldsymbol{x}_k + (h_k/6)(\boldsymbol{f}_k + 4\boldsymbol{f}_m + \boldsymbol{f}_{k+1}) \tag{32}$$

where for $k = 1, 2, \ldots, N-1$,

$$\boldsymbol{x}_m = \tfrac{1}{2}(\boldsymbol{x}_{k+1} + \boldsymbol{x}_k) - (h_k/8)(\boldsymbol{f}_{k+1} - \boldsymbol{f}_k) \tag{33}$$

$$\boldsymbol{u}_m = \tfrac{1}{2}(\boldsymbol{u}_{k+1} + \boldsymbol{u}_k) \tag{34}$$

$$t_m = \tfrac{1}{2}(t_{k+1} + t_k) \tag{35}$$

$$\boldsymbol{f}_k = \boldsymbol{f}(\boldsymbol{x}_k, \boldsymbol{u}_k, t_k) \tag{36}$$

$$\boldsymbol{f}_{k+1} = \boldsymbol{f}(\boldsymbol{x}_{k+1}, \boldsymbol{u}_{k+1}, t_{k+1}) \tag{37}$$

$$\boldsymbol{f}_m = \boldsymbol{f}(\boldsymbol{x}_m, \boldsymbol{u}_m, t_m) \tag{38}$$

The path constraint in Eq. (26) is converted into

$$\boldsymbol{S}(\boldsymbol{x}_k, \boldsymbol{u}_k, t_k) \geq 0 \tag{39}$$

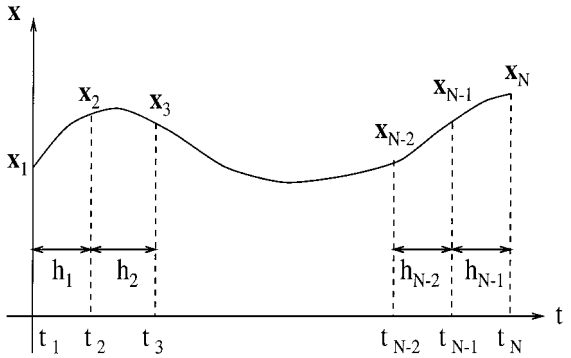

Fig. 2 Conversion of a continuous variable into parameters.

for $k = 1, 2, \ldots, N$; the initial condition constraint in Eq. (25) is converted into

$$\varphi(\boldsymbol{x}_1, t_1) \geq 0 \tag{40}$$

and the terminal constraint in Eq. (27) is converted into

$$\psi(\boldsymbol{x}_N, t_N) \geq 0 \tag{41}$$

where all vector inequalities are enforced component by component.

Putting all of the unknown variables together, we have

$$\boldsymbol{X}^T = \left[x_1^1, \ldots, x_N^1, \ldots, x_1^n, \ldots, x_N^n, u_1^1, \ldots, u_N^1, \ldots, u_1^m, \ldots, u_N^m, t_f\right] \tag{42}$$

All of the converted constraints are either linear or nonlinear functions of the parameter vector $\boldsymbol{X}$. As a result, the original nonlinear optimal control problem is approximated by the following parameter optimization problem:

$$\min_{X} \phi(\boldsymbol{X}) \tag{43}$$

subject to

$$\boldsymbol{L}_b \leq \begin{Bmatrix} \boldsymbol{X} \\ A\boldsymbol{X} \\ c(\boldsymbol{X}) \end{Bmatrix} \leq \boldsymbol{U}_b \tag{44}$$

This problem can be solved by the software NPSOL.[44] Strictly speaking, the converted problem is an approximation to the original optimal control problem. As the number of nodes becomes sufficiently large, this approximation often converges to the original problem.

In this paper, analytical gradients are provided for objective functions. Numerical differences are used for estimating gradients of the constraint functions. There are $(n+m)N+1$ solution parameters and $n(N-1)$ nonlinear constraints from the dynamic equations. There is no linear constraint. Different number of time interval divisions and initial guesses are used. The following results are obtained with $N = 21$.

Required Ranges with Heading Control

There are basically three control authorities for commercial aircraft: heading, speed, and altitude. These control authorities can be used singly or in combinations. This section examines required ranges for conflict resolutions using heading control only during en route flight.

With the use of heading control, it can be assumed that the two aircraft involved in a potential conflict are in constant speed coaltitude level flights. Mathematically, $V_i = \text{const}$ and $\gamma_i = 0$ for $i = 1, 2$, and $\Theta = 0$. It is further assumed that $V_1 = V_2$. The simplified and normalized equations are

$$\bar{R}' = \cos(\beta - \psi_r) - \cos\beta \tag{45}$$

$$\beta' = (1/\bar{R})[-\sin(\beta - \psi_r) + \sin\beta] - \tan\phi_1 \tag{46}$$

$$\psi_r' = \tan\phi_2 - \tan\phi_1 \tag{47}$$

where $V_c = V_1 = V_2$.

In these equations, the state variables are $[\bar{R},\ \beta,\ \psi_r]$. For noncooperative maneuvers, ϕ_1 is used as the control variable and $\phi_2 \equiv 0$. For cooperative maneuvers, both ϕ_1 and ϕ_2 are used as control variables.

The bank angle during a turn is limited by both the load factor and passenger comfort. The maximum load factor can be stall limited, structure limited, or thrust limited. It is always limited by thrust during normal operations of commercial aircraft. During a cruise flight, the thrust-limited load factor corresponds to $\phi_{\max} = 45$ deg for a typical commercial aircraft. On the other hand, passenger comfort limits bank angle to about 20–30 deg. In this study, it is assumed that $\phi_{\max} = 30$ deg.

The minimum range for the initiation of conflict resolution maneuvers for a given relative heading angle represents the condition from which proper conflict avoidance maneuvers would be barely sufficient to avoid a potential conflict. This minimum range can be determined from an optimal control problem. Mathematically,

$$\min_{\phi_1, \phi_2, \bar{R}_0, \tau_f} I = \bar{R}_0 \tag{48}$$

subject to Eqs. (45–47), path constraints

$$\bar{R} \geq \bar{a} \tag{49}$$

$$|\phi| \leq \phi_{\max} \tag{50}$$

and the terminal constraint

$$\bar{R}'(\tau_f) = \cos(\beta_f - \psi_{rf}) - \cos\beta_f \geq 0 \tag{51}$$

As initial conditions of the problem, $\bar{R}_0$ is open and is optimized in the solution, β_0 is fixed and chosen from [0, 180 deg] due to the problem symmetry, and ψ_{r0} is selected to make the problem meaningful:

$$\bar{R}_0' = \cos(\beta_0 - \psi_{r0}) - \cos\beta_0 < 0 \tag{52}$$

The problem is meaningful if there exists a potential conflict. The Appendix discusses choices of ψ_{r0} that satisfy Eq. (52) for given values of β_0.

Solutions of the preceding problem are in the form of $\bar{R}_{\min}(\beta_0, \psi_{r0})$. The required range for a given β_0 is then determined from

$$\bar{\mathcal{R}}(\beta_0) \triangleq \max_{\psi_{r0}} \bar{R}_{\min}(\beta_0, \psi_{r0}) = \max_{\psi_{r0}} \min_{u(t), t_f} \bar{R}_0 = \bar{R}_{\min}\left(\beta_0, \psi_{r0}^*\right) \tag{53}$$

This problem in Eq. (53) is solved as follows. For a given value of β_0, an interval of ψ_{r0} values that satisfy Eq. (52) is first determined from the Appendix. For each selected value of ψ_{r0} within this interval, the problem in Eq. (48) is solved using NPSOL. A bisection method is used on ψ_{r0} to determine ψ_{r0}^* that yields the maximum minimum initial range in Eq. (53). The bisection process is terminated when neighboring values of $\bar{\mathcal{R}}(\beta_0)$ are within 1% of $\bar{\mathcal{R}}(\beta_0)$.

Figure 3 shows contours of required ranges with heading control, as functions of the bearing angle. The bearing angle of $\beta = 0$ corresponds to the head-on conflict scenario and requires the largest range for conflict resolutions than all other values of β. For the noncooperative case, AC_1 should maneuver at least 15.22 n mile from AC_2 in a head-on encounter. For the cooperative case, both aircraft should maneuver when the two aircraft are at least 11.5 n mile apart in a head-on encounter. As the magnitude of the bearing angle increases, the relative speed of the two aircraft decreases, resulting in smaller required ranges. At $\beta = 180$ deg, the required range coincides with the minimum horizontal separation of 5 n mile. Clearly,

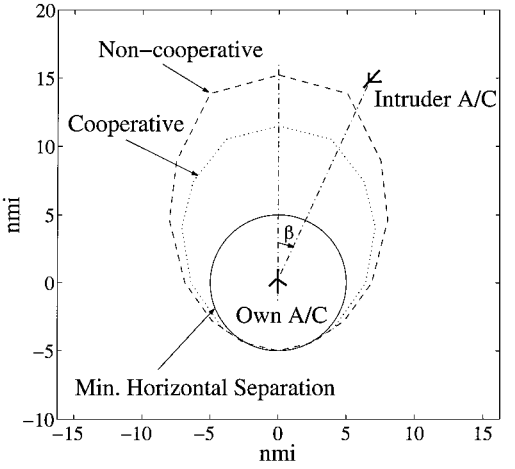

Fig. 3 Contours of required ranges with heading control.

cooperation of the two aircraft become important in reducing required ranges for close to head-on conflict scenarios. For tail-chasing types of conflicts, differences between cooperative and noncooperative maneuvers are not significant. Cooperative maneuvers require both aircraft to take corrective actions and, thus, have more controller/pilot workloads than noncooperative maneuvers. Therefore, it is better to employ a noncooperative strategy if it does not make too much difference from the cooperative strategy.

Optimal banking control strategies corresponding to required ranges exhibit bang–bang behaviors. Bank angles take values at ±30 deg. Different initial guesses of bank angles are used in solving the optimal control problem in Eq. (48), to determine which bound yields $\bar{R}_{\min}(\beta_0, \psi_{r0})$ for given β_0 and ψ_{r0}. With a noncooperative strategy, AC_1 can either bank to the left or to the right, depending on the orientation of AC_2. With a cooperative strategy, there are four combinations of banking strategies for the two aircraft, namely, (±30, ±30 deg). The optimal combination depends on specific aircraft conditions. Determinations of optimal banking rules are beyond the scope of the current paper.

Figure 4 shows the aircraft trajectories during the resolution of a head-on conflict with cooperative heading controls. This case corresponds to the point on the required range contour at $\beta = 0$ in Fig. 3, where $\psi^*_{r0} = 180$ deg. In this example, both aircraft turn to the right with the maximum allowed bank angle of 30 deg. In this case of $\beta = 0$ and $\psi^*_{r0} = 180$ deg, the two aircraft could equally both bank to the left.

Figure 5 shows the aircraft trajectories corresponding to $\beta =$ 50 deg on the required range contour with cooperative maneuvers. The banking directions shown are optimal. In this case, $\psi^*_{r0} =$ 255 deg. It seemed at the beginning that two types of ψ_{r0} might correspond to the solutions in Eq. (53). The first type is given by

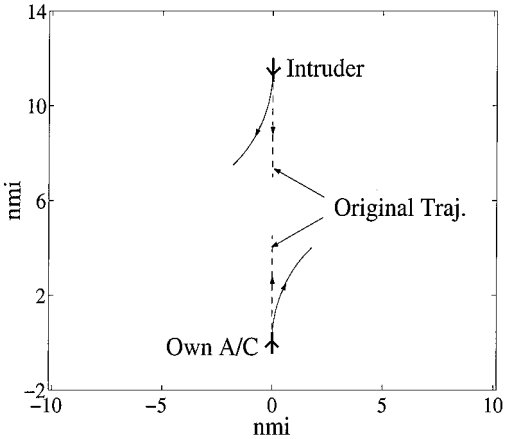

Fig. 4 Cooperative conflict resolution using heading control: $\beta_0 = 0$ and $\psi^*_{r0} = 180$ deg.

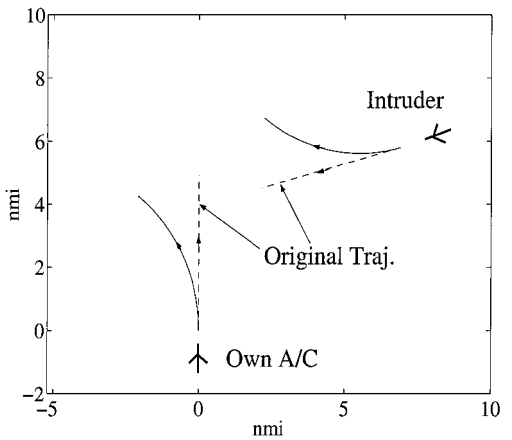

Fig. 5 Cooperative conflict resolution using heading control: $\beta_0 =$ 50 deg and $\psi^*_{r0} = 255$ deg.

Eq. (A3) in the Appendix that produces the most negative initial approach rate of the two aircraft. The other type would produce a direct collision of the two aircraft in the original flight paths. During the numerical solutions of the problem in Eq. (53), it is found that in general neither type of ψ_{r0} maximizes $\bar{R}_{\min}(\beta_0, \psi_{r0})$.

Required Ranges with Speed Control

Using speed control alone does not affect the geometric shapes of flight paths. It is assumed that $\psi_i =$ const and $\gamma_i = 0$ for $i = 1, 2$, and $h_1 = h_2$. These assumptions determine $\phi_i = 0$, $L_i = W_i$, and $\Theta = 0$. From Eq. (18), we have

$$D/W = (\rho S/2W)V^2 C_D(C_L) = \eta \bar{V}^2 C_D(C_L) \tag{54}$$

where

$$\eta \triangleq (\rho S/2W)V_c^2 \tag{55}$$

C_L can be calculated from $L = W$ using Eq. (17),

$$C_L = (2W/\rho S)(1/V^2) = (1/\eta)(1/\bar{V}^2) \tag{56}$$

Then, C_D can be calculated from Eq. (19).

The simplified and normalized equations are given by

$$\bar{R}' = \bar{V}_2 \cos(\beta - \psi_{r0}) - \bar{V}_1 \cos\beta \tag{57}$$

$$\beta' = [-\bar{V}_2 \sin(\beta - \psi_{r0}) + \bar{V}_1 \sin(\beta)]/\bar{R} \tag{58}$$

$$\bar{V}_1' = \kappa_1 (T_1/W_1)_{\max} - \eta \bar{V}_1^2 C_D(\bar{V}_1) \tag{59}$$

$$\bar{V}_2' = \kappa_2 (T_2/W_2)_{\max} - \eta \bar{V}_2^2 C_D(\bar{V}_2) \tag{60}$$

where $V_c = V_{10} = V_{20}$. Thrust settings κ_1 and κ_2 are directly used as control variables because the time needed for engine thrust spooling is usually much shorter than the time needed for conflict avoidance maneuvers. For noncooperative maneuvers, κ_1 is used as the control variable and κ_2 is such that $\bar{V}_2' = 0$. For cooperative maneuvers, both κ_1 and κ_2 are used as control variables.

The thrust setting κ (in percent) is constrained between idle (3%) and full (100%). In particular, the steady-state cruise condition corresponds to $\kappa = 77\%$. However, the use of idle thrust during cruising flight would produce an excessive deceleration.[38] Therefore, it is imposed that

$$0.5 \le \kappa_1, \kappa_2 \le 1 \tag{61}$$

In addition, the following constraints are imposed on speed variations:

$$|\bar{V}_1 - \bar{V}_{10}| \le \Delta\bar{V} \tag{62}$$

$$|\bar{V}_2 - \bar{V}_{20}| \le \Delta\bar{V} \tag{63}$$

Appropriate choices of increment speed ΔV can guarantee that the lift coefficient stays within appropriate limits.

The minimum range for the initiation of conflict resolution maneuvers at a specific relative heading angle can be obtained from the following optimal control problem:

$$\min_{\kappa_1, \kappa_2, \bar{R}_0, \tau_f} I = \bar{R}_0 \tag{64}$$

subject to Eqs. (57–60), path constraints in Eqs. (61–63) and Eq. (49), and the terminal constraint

$$\bar{R}'(\tau_f) = [\bar{V}_2 \cos(\beta - \psi_r) - \bar{V}_1 \cos\beta]_{\tau = \tau_f} \ge 0 \tag{65}$$

As initial conditions of the problem, $\bar{R}_0$ is open, β_0 is selected from [0, 180 deg], and

$$\bar{V}_{10} = 1.0 \tag{66}$$

$$\bar{V}_{20} = 1.0 \tag{67}$$

The initial relative heading ψ_{r0} is selected within [0, 360 deg] that satisfies Eq. (52) according to the Appendix. The required ranges are determined similarly to those with heading control.

Figure 6 shows contours of required ranges for conflict resolutions with speed control, as functions of the bearing angle. Required ranges with speed control have open ends in the front, corresponding to head-on conflict scenarios. This is because that without changing courses, speed control alone cannot avoid a head-on conflict. Overall, required ranges with speed control are extremely large for close to head-on encounters compared with those with heading control. Therefore, speed changes are ineffective in resolving potential conflicts in close to head-on encounters. For close to tail-chasing encounters, on the other hand, speed changes can be effective. Cooperation of the two aircraft helps to reduce the required ranges to a certain extent. In addition, the use of a larger speed increment ΔV results in smaller required ranges.

Optimal thrusting control strategies at required range contour boundaries also exhibit bang–bang behaviors. Again, different initial guesses of thrust settings are used to obtain global solutions in solving the problem in Eq. (64). With a noncooperative strategy, AC_1 should either accelerate or decelerate maximally until the aircraft reaches the specified airspeed bounds. For points on the required range contour, AC_1 always accelerates to avoid AC_2. With a cooperative strategy, one aircraft accelerates with $\kappa = 1$ while the other aircraft decelerates with $\kappa = 0.5$ [refer to Eq. (61)]. Exactly which aircraft accelerates depends on the relative orientations of the two aircraft. Figures 7a and 7b show cooperative conflict resolution trajectories at the point on the required range contour boundary in Fig. 6 with $\beta = 70$ deg. In this case, AC_1 slows down by $\Delta V = 50$ kn, whereas AC_2 speeds up by $\Delta V = 50$ kn. The relative heading angle that produces the maximum $\bar{R}_{\min}$ is $\psi^*_{r0} = 320$ deg.

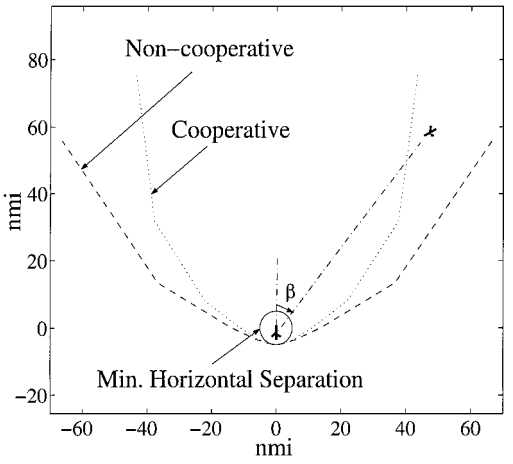

Fig. 6 Contours of required ranges with speed control, ΔV = 50 kn.

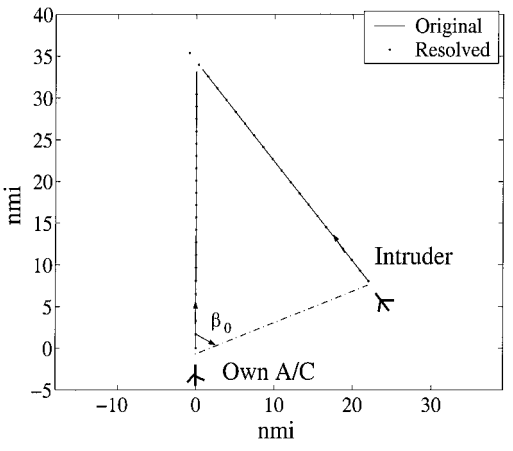

Fig. 7a Cooperative conflict resolution using speed control: β_0 = 70 deg and ψ^*_{r0} = 320 deg, horizontal path.

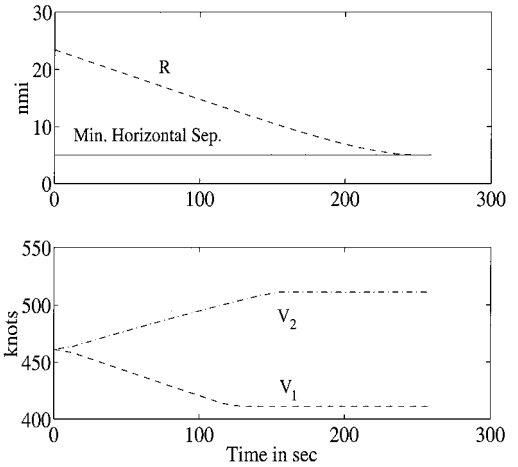

Fig. 7b Cooperative conflict resolution using speed control: β_0 = 70 deg and ψ^*_{r0} = 320 deg, range and speed.

Required Ranges with Altitude Control

With altitude control only, it is assumed that both aircraft stay in their original headings and speeds. Aircraft can change flight-path angles and altitude levels to prevent a potential conflict. Therefore, $\psi_i = \psi_{i0}$ and $\dot{V}_i = 0$, for $i = 1, 2$. It is assumed that $V_1 = V_2$.

In calculating required ranges with altitude control, flight-path angles can be used as control variables. For commercial flights, changes of flight-path angles take much less time than needed for a conflict resolution maneuver. Constraints on flight-path angles are imposed by thrusting capabilities and passenger comforts. Maintaining a constant speed requires

$$T_{\min} \le T = D + W \sin\gamma \le T_{\max}$$

which leads to

$$[(T - D)/W]_{\min} \le \sin\gamma \le [(T - D)/W]_{\max}$$

Using extreme thrust settings of 100 and 3% (full and idle, respectively), we obtain[38]

$$-3.7 \le \gamma \le 1.1$$

in degrees. On the other hand, passenger comforts often dictate

$$-3 \le \gamma \le 3$$

in degrees. As a result,

$$-3.0 \le \gamma \le 1.1 \tag{68}$$

Proper choices of solution variables can improve numerical convergences of optimization problems and can also lead to simplified solutions. Equations (14–16) represent the time rates of inertial positions of AC_1. They equally apply to AC_2 when all of the subscripts are replaced by 2. By the differentiating of the right-hand sides of Eqs. (4–6), one obtains the relative aircraft equations of motion in an inertial frame of reference. With normalized variables,

$$\Delta\bar{x}' = \cos\gamma_2 \sin\psi_{20} - \cos\gamma_1 \sin\psi_{10} \tag{69}$$

$$\Delta\bar{y}' = \cos\gamma_2 \cos\psi_{20} - \cos\gamma_1 \cos\psi_{10} \tag{70}$$

$$\Delta\bar{h}' = \sin\gamma_2 - \sin\gamma_1 \tag{71}$$

Define a transformation

$$z_1 = \Delta\bar{x} \cos\psi_{10} - \Delta\bar{y} \sin\psi_{10} \tag{72}$$

$$z_2 = \Delta\bar{x} \sin\psi_{10} + \Delta\bar{y} \cos\psi_{10} \tag{73}$$

$$z = (a/b)\Delta\bar{h} \tag{74}$$

We have

$$z_1' = \cos\gamma_2 \sin\psi_{r0} \approx \sin\psi_{r0} \tag{75}$$

$$z_2' = \cos\gamma_2 \cos\psi_{r0} - \cos\gamma_1 \approx \cos\psi_{r0} - 1 \tag{76}$$

$$z' = (a/b)(\sin\gamma_2 - \sin\gamma_1) = u_2 - u_1 \triangleq u \tag{77}$$

where

$$u_2 \triangleq (a/b)\sin\gamma_2 \tag{78}$$

$$u_1 \triangleq (a/b)\sin\gamma_1 \tag{79}$$

The newly defined variables z_1 and z_2 relate to the horizontal range in the polar coordinates and the bearing angle through

$$z_1 = \bar{r}\sin\beta \tag{80}$$

$$z_2 = \bar{r}\cos\beta \tag{81}$$

The relative range $\bar{R}$ and the elevation angle Θ can be determined from

$$\bar{R} = \sqrt{z_1^2 + z_2^2 + [(b/a)z]^2} = \sqrt{\bar{r}^2 + [(b/a)z]^2} \tag{82}$$

$$\sin\Theta = \Delta\bar{h}/\bar{R} = (\bar{b}/\bar{a})(z/\bar{R}) \tag{83}$$

The condition of successful conflict avoidance in Eq. (21) can be stated as

$$\bar{r}^2/\bar{a}^2 + [(\Delta\bar{h})^2/\bar{b}^2] \geq 1$$

or

$$\sqrt{z_1^2 + z_2^2 + z^2} \geq \bar{a} \tag{84}$$

during all times.

Because for a given $\Delta\bar{h}_0$ and thus given z_0,

$$\min\ \bar{R}_0 \Leftrightarrow \min\sqrt{z_{10}^2 + z_{20}^2} \Leftrightarrow \min\ \bar{r}_0$$

the minimum range for the initiation of conflict resolution maneuvers at a specific relative heading angle can be determined from the following optimal control problem:

$$\min_{\bar{r}_0, u, \tau_f} I = \sqrt{z_{10}^2 + z_{20}^2} = \bar{r}_0 \tag{85}$$

subject to Eqs. (75–77), bounds on the control u

$$u_{\min} \leq u \leq u_{\max} \tag{86}$$

and terminal constraints at τ_f

$$z_1^2(\tau_f) + z_2^2(\tau_f) + z^2(\tau_f) \geq \bar{a}^2 \tag{87}$$

$$(z_1 z_1' + z_2 z_2' + z z')_{\tau_f} = 0 \tag{88}$$

Using the calculus of variations, it can be shown that this problem results in bang–bang control. Thus, the control u is constant and stays at bounds. From Eqs. (75–77),

$$z_1 = z_{10} + \sin\psi_{r0}\tau = \bar{r}_0\sin\beta_0 + \sin\psi_{r0}\tau \tag{89}$$

$$z_2 = z_{20} + (\cos\psi_{r0} - 1)\tau = \bar{r}_0\cos\beta_0 + (\cos\psi_{r0} - 1)\tau \tag{90}$$

$$z = z_0 + u\tau \tag{91}$$

Substituting these results into the terminal constraint in Eq. (88) yields

$$\tau_f = -\frac{\bar{r}_0[\cos(\beta_0 - \psi_{r0}) - \cos\beta_0] + z_0 u}{2(1 - \cos\psi_{r0}) + u^2} = -\frac{\bar{r}_0\bar{r}_0' + z_0 u}{2(1 - \cos\psi_{r0}) + u^2} \tag{92}$$

where

$$\bar{r}_0' = \cos(\beta_0 - \psi_{r0}) - \cos\beta_0 \tag{93}$$

To make the problem meaningful, it is required that

$$\bar{r}_0\bar{r}_0' + z_0 z_0' = \bar{r}_0\bar{r}_0' + z_0 u < 0 \tag{94}$$

$$\sqrt{\bar{r}_0^2 + z_0^2} \geq \bar{a} \tag{95}$$

Applying Eq. (92) into the other terminal constraint in Eq. (87), we obtain

$$\left(\bar{r}_0^2 + z_0^2 - \bar{a}^2\right)\left[2(1 - \cos\psi_{r0}) + u^2\right] - (\bar{r}_0\bar{r}_0' + z_0 u)^2 \geq 0 \tag{96}$$

Because of Eq. (94), Eq. (96) leads to

$$\sqrt{\left(\bar{r}_0^2 + z_0^2 - \bar{a}^2\right)\left[2(1 - \cos\psi_{r0}) + u^2\right]} \geq -(\bar{r}_0\bar{r}_0' + z_0 u) \tag{97}$$

Therefore, the optimal control problem in Eqs. (85–88) becomes a parameter optimization problem with the cost function in Eq. (85) and constraints in Eqs. (86), (95), and (97). As a result, the required ranges for conflict resolutions with altitude control can be determined from the following static game:

$$\max_{\psi_{r0}} \min_{u}\ \bar{r}_0 \tag{98}$$

subject to Eqs. (86), (95), and (97).

For noncooperative maneuvers, γ_1, thus, u_1, is the only control variable and $\gamma_2 = 0$. Combining Eqs. (68), (77), and (79), we have (in degrees)

$$u = -u_1 \qquad u_{\min} = -(a/b)\sin 1.1 \qquad u_{\max} = (a/b)\sin 3.0 \tag{99}$$

For cooperative maneuvers, both γ_1 and γ_2 are control variables, and

$$u = u_2 - u_1 \qquad u_{\max} = -u_{\min} = (a/b)(\sin 1.1 + \sin 3.0) \tag{100}$$

Solution process of the maximization part is similar to the required range calculations in the preceding sections.

Figure 8 shows contours of required ranges with altitude control, as functions of the bearing angle. The bearing angle of $\beta = 0$ corresponds to the head-on conflict scenario and requires the largest response range than all other bearing angles. For the noncooperative case, AC_1 should maneuver at least 13.54 n mile from AC_2 in a head-on encounter. For the cooperative case, both aircraft should maneuver when the two aircraft are at least 10.47 n mile apart in a head-on encounter. As the magnitude of the bearing angle increases, the relative speed of the two aircraft decreases, resulting in smaller

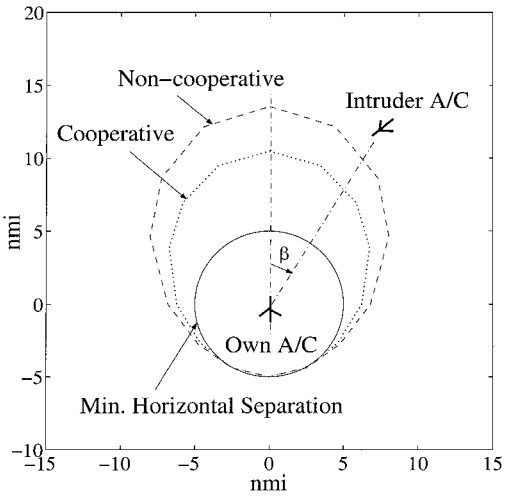

Fig. 8 Contours of required ranges with altitude control: dh_0 = 0.

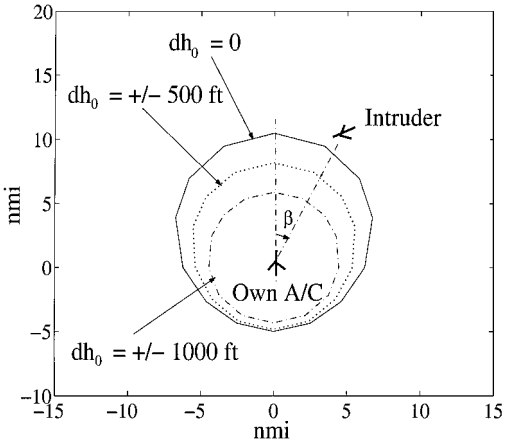

Fig. 9 Contours of required ranges with cooperative altitude control: effects of dh_0.

required ranges. At $\beta = 180$ deg, the required range becomes the same as the minimum horizontal separation standard of 5 n mile. As in the case with heading control, cooperation of the two aircraft involved becomes important in reducing required ranges for close to head-on conflict scenarios. For tail-chasing types of conflicts, differences between cooperative and noncooperative maneuvers are not significant.

Let us now examine the differences between required ranges with heading control in Fig. 3 and those with altitude control in Fig. 8. With heading controls, the required ranges in a head-on encounter are slightly larger than those with altitude controls, suggesting that altitude controls are slightly more effective than heading controls in resolving head-on conflict encounters. Overall, heading control and altitude control are comparable in terms of effectiveness of conflict resolutions, despite that the horizontal separation requirement (5 n mile en route) is much larger than the vertical separation requirement (2000 ft over flight level 290).

When altitude controls are used, the required ranges for conflict resolutions also depend on the initial altitude difference between AC_1 and AC_2. Figure 9 shows contours of required ranges with cooperative altitude controls at different initial vertical separations. With cooperative maneuvers, the required range contour is symmetric with respect to the horizontal plane of $\Theta = 0$. As the initial vertical separation increases in magnitude, the range required to resolve a potential conflict decreases. The required ranges with cooperative altitude controls in the case of $dh_0 = 1000$ ft are smaller than the minimum horizontal separation standard of 5 n mile. This is caused by the ellipsoidal approximation of the current minimum separation requirements in Eq. (21). With noncooperative maneuvers, the required range contour is not symmetric with respect to the horizontal plane of $\Theta = 0$ because the upper and lower bounds on flight-path angles are not symmetric, as indicated by Eq. (68). Details are omitted.

Optimal flight path-angle strategies at the required range contour boundaries again exhibit bang–bang behaviors. Different initial guesses of flight-path angles are used to obtain global solutions in solving the problem in Eq. (98). With a noncooperative strategy, AC_1 should either climb at a maximum of 1.1 deg or descend at -3.0 deg, depending on the initial altitude difference dh_0. With a cooperative strategy, there are two equivalent optimal solutions for $h_{20} = h_{10}$. Either aircraft can climb at 1.1 deg while the other aircraft descends at -3.0 deg. If $h_{20} > h_{10}$, the AC_2 always climbs and AC_1 always descends. It is the opposite if $h_{20} < h_{10}$. If other factors such as fuel economy are considered, these conclusions may be altered.

Comment

Problems formulated in this paper can be extended to account for effects of pilot/controller response times, communication delays, etc. To this end, dynamic models of these effects can be added to the equations of motion. Inclusion of these effects will likely increase the sizes of required range contours.

Conclusions

This paper presents a systematic approach to estimating ranges required for resolutions of two-aircraft conflicts. Point-mass aircraft models with a single control authority are employed. Aircraft control is assumed to be heading, speed, or altitude. Performance characteristics of a typical commercial aircraft are used. Optimal control problems are formulated to minimize the initial range between two aircraft subject to aircraft dynamics and constraints from aircraft performances and passenger comforts, so that if immediate conflict resolution actions are taken, the potential conflict is barely resolved during subsequent motions. Required ranges for conflict resolutions are then estimated by varying the initial relative heading angle to produce the largest minimum initial range for each specified bearing angle. Required range contours are calculated for the individual uses of heading, speed, and altitude control. Both cooperative maneuvers and noncooperative maneuvers are examined.

The optimal control problems are converted to parameter optimizations via a collocation approach and are solved numerically. In the case of altitude control, the problem is reduced to a static game and is solved numerically as a series of parameter optimization problems. For the examples presented in this paper, en route flight is assumed.

Required ranges with heading control and with altitude control are similar, suggesting that heading control and altitude control are comparably effective in resolving potential conflicts. Required range contours with speed control have open front ends for small bearing angles and are overall much larger than those with heading or altitude control. Therefore, heading control and altitude control are more effective than speed control in resolving conflicts. Especially, speed control alone is not sufficient to resolve potential conflicts in head-on encounters. Speed control may be used to resolve conflicts in tail-chasing encounters. For a given control authority, it requires a shorter range to resolve a potential conflict in tail-chasing encounters than in head-on encounters. Cooperative maneuvers are more effective than noncooperative maneuvers in resolving head-on conflict encounters. When an intruder aircraft approaches from behind the own aircraft, the benefits of cooperative maneuvers over noncooperative maneuvers become small.

Appendix: Determination of Initial Relative Headings

Given β_0, determine values of ψ_{r0} for which the time derivative of the initial range is negative, so that the ensuing optimization problem is meaningful. Omitting subscripts $(\,)_0$ for simplicity, the problem here is to determine values of ψ_r for a given β, such that

$$f(\psi_r) = \cos(\beta - \psi_r) - \cos\beta < 0 \tag{A1}$$

It is assumed that $|\beta| \le \pi$ and $0 \le \psi_r \le 2\pi$.

For $|\beta| = \pi$, the initial separation rate is nonnegative so that the problem of required range calculation is not meaningful. At this point, the required range coincides with the minimum separation standard. For β in the range of $0 \le |\beta| < \pi$, appropriate values of ψ_r that make the initial separation rate negative are given by

$$2\beta < \psi_r < 2\pi \tag{A2}$$

where the value of ψ_r that makes the initial separation rate most negative is given by

$$\psi_r^* = \beta + \pi \tag{A3}$$

which leads to

$$f = -1 - \cos\beta \tag{A4}$$

Acknowledgments

This research is supported by the Terminal Air Traffic Management Branch at NASA Ames Research Center under NCC2-990. The authors thank Klaus Well and anonymous reviewers for many constructive comments.

References

[1]Nolan, M. S., *Fundamentals of Air Traffic Control*, 2nd ed., Wadsworth, Belmont, CA, 1994, pp. 215–232.

[2]*Free Flight Implementation*, Final Rept. of Radio Technical Committee on Aeronautics (RTCA), Task Force 3, RTCA, Inc., Washington, DC, Oct. 1995.

[3]Erzberger, H., Davis, T. J., and Green, S. M., "Design of Center-TRACON Automation System," AGARD Guidance and Control Symposium on Machine Intelligence in Air Traffic Management, AGARD, May 1993.

[4]Erzberger, H., "Design Principles and Algorithms for Automated Air Traffic Management," Lecture Series 200 on Knowledge-Based Functions in Aerospace Systems, AGARD, Nov. 1995.

[5]Denery, D. G., and Erzberger, H., "The Center-TRACON Automation System: Simulation and Field Testing," NASA TM 110366, Aug. 1995.

[6]Davis, T. J., Erzberger, H., Green, S. M., and Nedell, W., "Design and Evaluation of Air Traffic Control Final Approach Spacing Tool," *Journal of Guidance, Control, and Dynamics,* Vol. 14, No. 4, 1991, pp. 848–854.

[7]Davis, T. J., Krzeczowski, K. J., and Bergh, C., "The Final Approach Spacing Tool," International Federation of Automatic Control Symposium on Automatic Control in Aerospace, Sept. 1994.

[8]Erzberger, H., and Tobias, L., "A Time-Based Concept for Terminal-Area Traffic Management," NASA TM 88243, April 1986.

[9]Erzberger, H., "Automation of On-Board Flightpath Management," NASA TM 84212, Dec. 1981.

[10]Slattery, R. A., and Zhao, Y., "Trajectory Synthesis in Air Traffic Automation," *Journal of Guidance, Control, and Dynamics*, Vol. 20, No. 2, 1997, pp. 232–238.

[11]Paielli, R. A., and Erzberger, H., "Conflict Probability Estimation for Free Flight," *Journal of Guidance, Control, and Dynamics*, Vol. 20, No. 3, 1997, pp. 588–596.

[12]Bergh, C. P., Krzeczowski, K. J., and Davis, T. J., "TRACON Aircraft Arrival Planning and Optimization Through Spatial Constraint Satisfaction," *Air Traffic Control Quarterly*, Vol. 3, No. 2, 1995, pp. 117–138.

[13]Slattery, R. A., and Green, S., "Conflict-Free Trajectory Planning for Air Traffic Control Automation," NASA TM-108790, Jan. 1994.

[14]Isaacson, D. R., and Erzberger, H., "Design of a Conflict Detection Algorithm for the Center TRACON Automation System," *Proceedings of the 16th AIAA/IEEE Digital Avionics Systems Conference*, IEEE Publications, Piscataway, NJ, 1997, pp. 9.3-1–9.3-9.

[15]Harman, W. H., "TCAS, A System for Preventing Midair Collisions," *Lincoln Laboratory Journal*, Vol. 2, No. 3, 1989, pp. 437–457.

[16]Williamson, T., and Spencer, N. A., "Development and Operation of the Traffic Alert and Collision Avoidance System (TCAS)," *Proceedings of the IEEE*, Vol. 77, No. 11, 1989, pp. 1735–1744.

[17]Walsh, J., and Wojciech, J., "TCAS in the 1990s," *Navigation: Journal of the Institute of Navigation*, Vol. 38, No. 4, 1991–1992, pp. 383–397.

[18]Burgess, D. W., Altman, S. I., and Wood, M. L., "TCAS: Maneuvering Aircraft in the Horizontal Plane," *Lincoln Laboratory Journal*, Vol. 7, No. 2, 1994, pp. 295–312.

[19]Carpenter, B., and Kuchar, J., "Probability-Based Collision Alerting Logic for Closely Spaced Parallel Approach," AIAA Paper 97-0222, 1997.

[20]Tomlin, C., Pappas, G. J., and Sastry, S., "Conflict Resolution for Air Traffic Management: A Study in Multiagent Hybrid System," *IEEE Transactions on Automatic Control*, Vol. 43, No. 4, 1998, pp. 509–521.

[21]Niedringhaus, W. P., "Maneuver Option Manager: Automated Simplification of Complex Air Traffic Control Problems," *IEEE Transactions on Systems, Man, and Cybernetics*, Vol. 22, No. 5, 1991, pp. 1047–1057.

[22]Irvine, R., "The Gears Conflict Resolution Algorithm," AIAA Paper 98-4236, Aug. 1998.

[23]Yang, L. C., and Kuchar, J. K., "Using Intent Information in Probabilistic Conflict Analysis," AIAA Paper 98-4237, Aug. 1998.

[24]Alliot, J.-M., Gruber, H., Joly, G., and Schoenauer, M., "Genetic Algorithms for Solving Air Traffic Control Conflicts," Inst. of Electrical and Electronics Engineers, Paper 1043-0989/93, 1993.

[25]Eby, M. S., "A Self-Organizational Approach for Resolving Air Traffic Conflict," *Lincoln Laboratory Journal*, Vol. 7, No. 2., 1994, pp. 239–254.

[26]Miura, A., Morikawa, H., and Mizumachi, M., "Aircraft Collision Avoidance with Potential Gradient—Ground-Based Avoidance for Horizontal Maneuvers," *Electronics and Communication in Japan, Pt. 3*, Vol. 78, No. 10, 1995, pp. 104–114.

[27]Zeghal, K., "A Review of Different Approaches Based on Forced Fields for Airborne Conflict Resolution," AIAA Paper 98-4240, Aug. 1998.

[28]Duong, V., and Zeghal, K., "Conflict Resolution Advisory for Autonomous Airborne Separation in Low-Density Airspace," *Proceedings of 36th IEEE Conference on Decision and Control*, Inst. of Electrical and Electronics Engineers, New York, 1997, pp. 2429–2434.

[29]Oh, J.-H., and Feron, E., "Primal-Dual Quadratic Programming Approach to Multiple Conflict Resolution," *Proceedings of the American Control Conference*, IEEE Publications, Piscataway, NJ, 1998, pp. 2802–2806.

[30]Oh, J.-H., and Feron, E., "Safety Certification of Air Traffic Conflict Resolution Algorithms Involving More Than Two Aircraft," *Proceedings of the American Control Conference*, IEEE Publications, Piscataway, NJ, 1998, pp. 2807–2811.

[31]Merz, A. W., "Optimal Aircraft Collision Avoidance," *Proceedings of the American Control Conference*, IEEE Publications, Piscataway, NJ, 1973, pp. 449–454.

[32]Krozel, J., and Peters, M., "Conflict Detection and Resolution for Free Flight," *Air Traffic Control Quarterly*, Vol. 5, No. 3, 1997, pp. 181–212.

[33]Zhao, Y., and Schultz, R. L., "Deterministic Resolution of Two Aircraft Conflict in Free Flight," AIAA Paper 97-3547, Aug. 1997.

[34]Ota, T., Nagati, M. G., and Lee, D. C., "Aircraft Collision Avoidance Trajectory Generation," AIAA Paper 98–4241, Aug. 1998.

[35]Kuo, V. H., "Conflict Resolutions and Alert Zone Estimation in Air Traffic Management," Ph.D. Dissertation, Dept. of Aerospace Engineering and Mechanics, Univ. of Minnesota, Minneapolis, MN, Jan. 1999.

[36]Menon, P. K. A., Sweriduk, G. D., and Sridhar, B., "Optimal Strategies for Free-Flight Air Traffic Conflict Resolution," *Journal of Guidance, Control, and Dynamics*, Vol. 22, No. 2, 1999, pp. 202–211.

[37]Jackson, M. R., Zhao, Y. J., and Slattery, R. A., "Sensitivity of Trajectory Prediction in Air Traffic Management," *Journal of Guidance, Control, and Dynamics*, Vol. 22, No. 2, 1999, pp. 219–228.

[38]Bilimoria, K., Sridhar, B., and Chatterji, G., "Effects of Conflict Resolution Maneuvers and Traffic Density on Free Flight," AIAA Paper 96-3767, July 1996.

[39]Menon, P. K. A., "Air Traffic Conflict Resolution Using Modern Control Theory," Research Rept., Optimal Synthesis, Inc., Palo Alto, CA, Oct. 1992.

[40]Bryson, A. E., Jr., *Dynamic Optimization*, Addison Wesley Longman, Reading, MA, 1999, Chaps. 2–4.

[41]Seywald, H., *Computational Optimal Control*, AIAA Short Course Notes, AIAA Guidance and Control Conf., Aug. 1998.

[42]Betts, J., "Survey of Numerical Methods for Trajectory Optimization," *Journal of Guidance, Control, and Dynamics*, Vol. 21, No. 2, 1998, pp. 193–207.

[43]Hull, D., "Conversion of Optimal Control Problems Into Parameter Optimization Problems," AIAA Paper 96-3812, July 1996.

[44]Gill, P. E., Murray, W., Saunders, M. A., and Wright, W., "NPSOL User's Manual," System Optimization Lab., TR SOL 86-2, Dept. of Operation Research, Stanford Univ., Stanford, CA, Jan. 1986.